

## Whole-Body Retention of Radioxenon

Herbert Susskind, Harold L. Atkins, Stanton H. Cohn, Kenneth J. Ellis, and Powell Richards

*Applied Science and Medical Departments,  
Brookhaven National Laboratory, Upton, New York*

*The total-body retention of  $^{127}\text{Xe}$ , and its variation with time following short, nonequilibrium periods of inhalation, were measured in vivo so as to refine dosimetry calculations. Radioactivity in the chest region and in the recirculating xenon-air mixture was measured continuously during re-breathing of the gas mixture and in the first 5 min of the immediate gas-washout period using a scintillation camera and shielded NaI detector, respectively. Subjects were then counted in a whole-body counter at varying time intervals until background levels were reached, usually in  $\sim 72$  hr. Five components of Xe clearance from the entire body were measured; they had biologic half-times of  $21.7 \pm 12.4$  sec,  $3.05 \pm 1.72$  min,  $0.40 \pm 0.11$  hr, and  $2.71 \pm 0.87$  hr, and a long-term component varied between 7.59 and 17.04 hr. The half-time of the last component correlated highly with the percent of total-body fat. After 10-min inhalations of the xenon-air mixture, approximately one-third of the total xenon was transferred to the body tissues, extrapolated back to the start of gas washout. Of this amount,  $\sim 13\%$  was associated with the slowest component of clearance.*

J Nucl Med 18: 462-471, 1977

Metabolic models are necessary for estimation of the radiation absorbed dose for human exposure to radioactive xenon, principally through the inhalation of low levels of radioactive xenon in routine clinical studies of lung ventilation and perfusion (1). Xenon has a number of radionuclides, but until recently  $^{133}\text{Xe}$  has been used almost exclusively for these regional lung-function studies. Xenon-133 decays by beta emission with a half-life of 5.3 days, and produces 81-keV photons at 37% abundance. More recently,  $^{127}\text{Xe}$  has become available, with a 36.4-day half-life. It is routinely produced in a  $^{133}\text{Cs}(p,2p5n)^{127}\text{Xe}$  reaction by proton irradiation of CsCl.\* Its 172-, 203-, and 375-keV photons are emitted at an abundance of over 100%, and are much closer to the optimum energy range for best spatial resolution with the scintillation camera.

Two values for the radiation dose from  $^{127}\text{Xe}$  have been cited in the literature (2,3), but without a statement of the assumptions used in their derivation. Goddard and Ackery (4) more recently have provided dosage calculations, but for lack of available data they had to assume values for certain parameters. In vitro data are available on the solu-

bilities and partition coefficients of xenon in human blood, fat, and other individual body constituents (5-12), but only two clinical studies of its retention and clearance from the body have been reported (13,14).

In order to refine dosimetry calculations, the total-body retention (TBR) of  $^{127}\text{Xe}$  and its variation with time following short, nonequilibrium periods of inhalation were measured in vivo. Also determined were the effective biologic half-times for the different rate components and their fractions in the body, as well as the ratio of concentrations of  $^{127}\text{Xe}$  distributed between fatty tissue and air after re-breathing a xenon-air mixture for 10 or for 30 min. The retention data were obtained by the Brookhaven whole-body counter, which can detect a body burden of as little as  $3 \times 10^{-4}$   $\mu\text{Ci}$   $^{127}\text{Xe}$ . Therefore, administered doses of less than 100  $\mu\text{Ci}$  of  $^{127}\text{Xe}$  per subject sufficed. The whole-body counter also automatically

Received Sept. 7, 1976; revision accepted Dec. 8, 1976.

For reprints contact: Herbert Susskind, Applied Science Dept., Brookhaven National Lab., Upton, NY 11973.

TABLE 1. PHYSICAL CHARACTERISTICS OF THE NORMAL SUBJECTS

Subject	Age, yr	Height, cm	Weight, kg	TBK, g*	LBM, kg†	BF, kg‡	% Body fat
1	44	157.9	58.18	113.6	44.10	14.08	24.2
2	49	172.2	74.55	144.9	56.25	18.25	24.5
3(F)	29	166.4	54.50	93.20	40.32	14.18	26.0
4	60	180.3	78.18	147.5	57.26	20.92	26.8
5A†	46	180.3	88.18	160.6	62.34	25.84	29.3
5B			93.64	155.9	60.52	33.12	35.4
6	58	180.3	84.09	137.2	53.26	30.83	36.7
7(F)	54	160.0	58.06	80.93	35.03	23.03	39.6
8(F)	61	160.5	50.00	68.36	29.57	20.43	40.8
9	43	180.3	122.3	186.3	72.32	49.98	40.9
10	59	175.5	113.6	158.3	61.45	52.15	46.0
11(F)	55	151.6	86.36	90.85	39.32	47.04	54.4
12(F)	44	166.4	139.1	117.3	50.74	88.36	63.5

\* TBK = Total-body potassium; 1 g K  $\approx$  0.39 kg LBM for males and  $\approx$  0.43 kg LBM for females.

† LBM = Lean body mass.

‡ BF = Body fat = Body weight - LBM.

|| % Body fat = (BF/body weight)  $\times$  100.

† Subject 5 was measured on two different occasions, and the body weight had changed.

corrected for photon attenuation due to differences in body build, and for the effects of geometrical distribution of radioactivity within the body (15).

#### EXPERIMENTAL

**Subjects.** Seven male and five female volunteers with no known pulmonary disease participated in the study. They ranged in age from 29 to 61 years, and in weight from 110 to 306 lb (Table 1). Their total-body fat content varied between 24 and 64% of the body weight, as determined by whole-body counting of  $^{40}\text{K}$  (TBK) for estimation of the lean body mass (LBM) (16,17). The body fat was defined as the difference between the body weight and LBM. In both sexes, the LBM/TBK ratio was relatively constant for the age span of the subjects, 1 g potassium being approximately equal to 0.39 kg LBM for males and 0.43 kg LBM for females (17).

**Methods.** Before each run, the whole-body background activity was measured and spirometry was performed to determine total lung capacity and functional residual capacity (FRC). The subject's average lung volume was determined from the sum of FRC plus half the tidal volume ( $V_T$ ). The actual amount of  $^{127}\text{Xe}$  introduced to the system was varied to maintain the average xenon concentration in the lungs relatively constant for all subjects.

Tidal volumes of the mixtures of  $^{127}\text{Xe}$  and air were rebreathed in a closed spirometer system for 10 min in each case to duplicate the time interval of a typical ventilation study. One subject (Subject 5) repeated the 10-min rebreathing run, while three subjects (Subjects 2, 9, and 10) repeated the study by rebreathing the mixture for 30 min. Two subjects rebreathed for 10 min a gas mixture containing about

nine times (Subject 4) and 65 times (Subject 6) the average  $^{127}\text{Xe}$  concentration.

The arrangement of the apparatus is shown schematically in Fig. 1, and Fig. 2 shows a subject at the start of a typical run. The subject, with nose clamped, sat upright and breathed through a rubber mouthpiece connected to the 10-liter rebreathing spirometer system.† Constant volume was maintained in the system by automatic replenishment of  $\text{O}_2$  and absorption of  $\text{CO}_2$  in soda lime. For six of the subjects, radioactivity was measured continuously in the chest region with a wide-field scintillation camera,‡ and in the recirculating air at the mouth with a shielded NaI detector, during the rebreathing period and the first 5 min of gas washout.

The required amount of  $^{127}\text{Xe}$  was injected from a gas-tight glass syringe into the rubber mouthpiece.

A calibrated sample volume of the gas mixture,  $\sim 8$  ml, was collected through a needle in the rubber

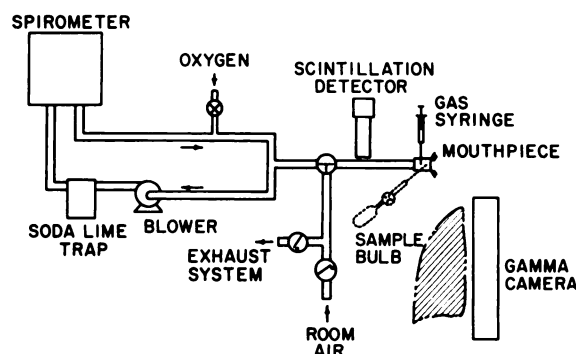
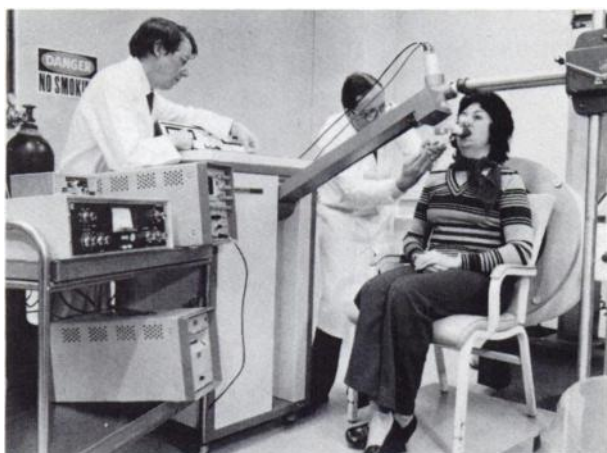
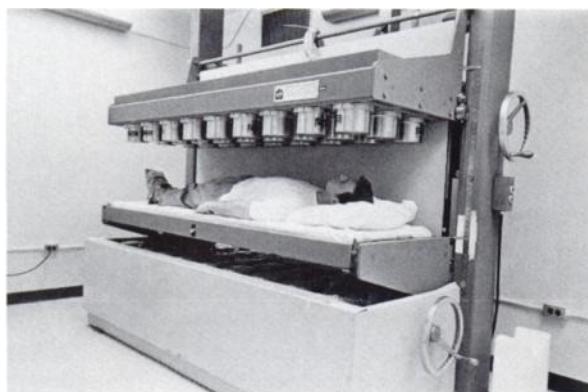


FIG. 1. Schematic representation of the apparatus used for rebreathing the xenon-air mixture and measuring the initial  $^{127}\text{Xe}$  uptake.



**FIG. 2.** Subject seated upright against scintillation camera and rebreathing the xenon-air mixture through a closed spirometer system. Shielded NaI detector is located near the mouthpiece. Xenon-127 is being injected into mouthpiece.



**FIG. 3.** Whole-body counter, showing upper bank of 27 NaI(Tl) detectors, in nine rows of three. Similar bank of detectors is beneath subject.

mouthpiece just before the start of gas washout. From this sample, the  $^{127}\text{Xe}$  concentration and its total activity in the lungs were determined with a Ge(Li) detector. The sample was also measured on the whole-body counter to determine the conversion factor from counts per minute to  $\mu\text{Ci}$  for  $^{127}\text{Xe}$ . This was possible because the whole-body counter has an invariant response to both the radionuclide distribution and the size of the body being measured (15).

In order to reduce the concentration of retained  $^{127}\text{Xe}$  to that measurable by the whole-body counter, the subject remained at the spirometer for the first 5 min of gas washout, inspiring room air and expiring into an exhaust vent. Measurements then commenced at the whole-body counter  $\sim 7$  min after the start of washout. The subjects were counted at varying time intervals until background levels were

reached, usually in  $\sim 72$  hr. The whole-body counter consists of two banks of 27 NaI(Tl) detectors each, arranged in a 3 (column)  $\times$  9 (row) grid array (Fig. 3). The subject lies on a bed, with the two banks equally spaced (71 cm total separation) above and below the bed during the measurements.

## RESULTS

The variation in  $^{127}\text{Xe}$  activity with time during a typical run (Subject 2), is shown in Fig. 4 for a 30-min rebreathing period and the first 5 min of gas washout. For the more usual 10-min rebreathing period, the slight increase in chest radioactivity and slight decrease in recirculating activity were not as readily noticeable. The xenon activity gradually decreased at a rate of  $\sim 1\%$ /min in the recirculating air, with a corresponding activity increase of  $\sim 0.9\%$ /min in the chest region. At such a time, the concentration of dissolved xenon in the blood will increase, and will be equal to the product of that in the lungs and the blood-to-air partition coefficient. Similarly, the concentrations of  $^{127}\text{Xe}$  in the chest region and elsewhere in the body will increase in accordance with their respective tissue-to-blood partition coefficients and rates of perfusion to those tissues. The retention data were resolved graphically into two components, using least-square fits. The two biologic half-times for Subject 2 from the start of gas washout were 35.9 sec and 14.8 min over the chest region, and in the recirculating air they were 13.1 sec and 8.16 min.

Similarly, the retention data from the whole-body

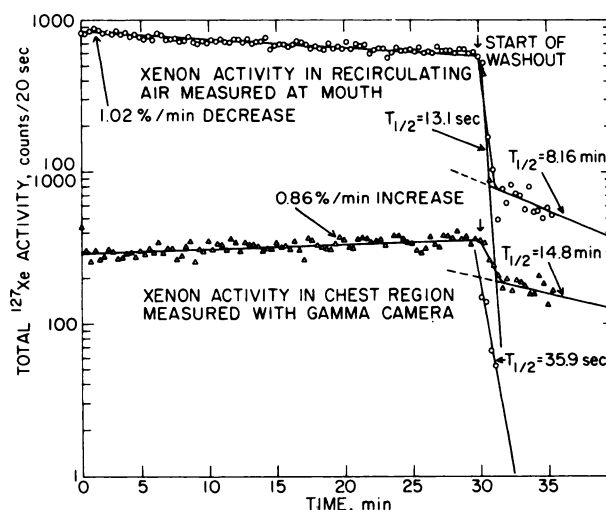


**FIG. 4.** Time course of  $^{127}\text{Xe}$  activity in Subject 2 during a typical run, here involving a 30-min rebreathing period and 5 min of gas washout; measured with scintillation camera and NaI detector. As  $^{127}\text{Xe}$  was taken up by the body, activity gradually increased in the chest region and decreased in the recirculating air. Retention data following gas washout were resolved into two components.

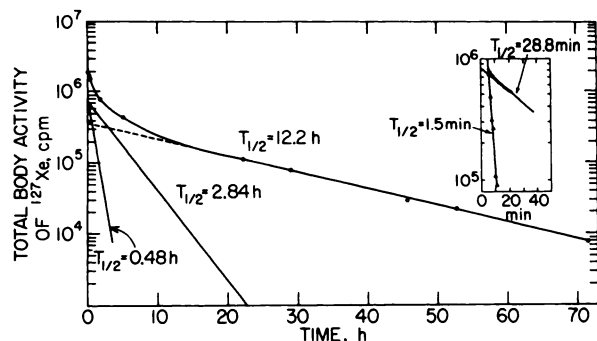


**FIG. 5.** Typical activity-time curve for Subject 10 measured with the whole-body counter, and three components into which it can be resolved in the time interval between 7 min and 72 hr after the start of gas washout (0.48 hr = 28.8 min). Insert, with the expanded time scale, shows a fourth component.

counter were resolved into a sum of exponential curves, using the SAAM-25 computer curve-fitting program (18). Figure 5 shows a typical activity-time curve (Subject 10) and three components into which it could be resolved in the time interval between 7 min and 72 hr after the start of gas washout. A fourth component, with a half-time of  $\sim 1.5$  min, can be seen in the insert with the expanded time scale. This component's half-time is of the same magnitude as the second of those measured with the scintillation camera and NaI detector during the first 5 min of gas washout.

The body-retention data indicated that a five-

component exponential curve best described the desaturation phase up to 72 hr after the start of gas washout (Table 2). The half-times of the first four components were independent of the subjects' physical characteristics, and remained constant at  $21.7 \pm 12.4$  sec,  $3.05 \pm 1.72$  min,  $0.40 \pm 0.11$  hr, and  $2.71 \pm 0.87$  hr, respectively. The fifth component depended on the percentage of total-body fat, and varied between 7.59 and 17.04 hr (Fig. 6).

Extrapolated values for total-body retention of  $^{127}\text{Xe}$  at the start of gas washout are shown in Table 3. Also shown are the intercepts for components 2 to 5, expressed as percent of TBR. No values could be obtained for component 1 because its rapid clearance prevented its measurement on the whole-body counter, and the scintillation camera viewed only the chest region. The average values for  $^{127}\text{Xe}$  uptake measured on the whole-body counter (components 3 to 5, only) were  $50.2 \pm 12.6$ ,  $33.7 \pm 9.8$ , and  $16.1 \pm 8.3\%$ , respectively.

#### DISCUSSION

The rate at which a tissue in the body stores or releases an inert gas depends upon the tissue-to-blood partition coefficient and the blood perfusion rate to that tissue (19). The basic process can be described by the Fick principle, in which the retention of gas in the tissue,  $Q(t)$ , at time  $t$  is

$$Q(t) = Q_0 e^{-\lambda t}$$

**TABLE 2.  $^{127}\text{Xe}$  CLEARANCE FROM THE BODY\***

Subject	% Body fat	Biologic half-time, $t_{1/2}\dagger$				
		Component 1 (sec)	Component 2 (min)	Component 3‡ (hr)	Component 4 (hr)	Component 5 (hr)
1	24.2			0.26	2.07	7.59
2	24.5	35.9	14.80	0.20	1.54	8.01
3(F)	26.0	nd	2.63	0.31	2.86	9.29
4	26.8			—	2.64	8.95
5A	29.3			0.37	3.09	8.30
5B	35.4	12.9	5.85	0.49	3.49	8.39
6	36.7			—	3.0	10.7
7(F)	39.6	16.2	2.67	0.45	2.66	10.15
8(F)	40.8			0.45	4.54	10.58
9	40.9	nd	2.97	0.52	1.10	11.20
10	46.0	nd	1.12	0.48	2.84	12.22
11(F)	54.4			0.42	3.17	13.27
12(F)	63.5			—	2.20	17.04
Mean		21.7	3.05	0.40	2.71	10.44
s.d.		12.4	1.72	0.11	0.87	2.61

\* Based on rebreathing a Xe-air mixture for 10 min.

† Components 1 and 2 were calculated from scintillation-camera measurements; the other three components from whole-body counter measurements only.

‡ Values not computed for Subjects 4, 6, and 12 because of insufficient data in first 2 hr of washout.

|| Value not included in calculating the mean and standard deviation.

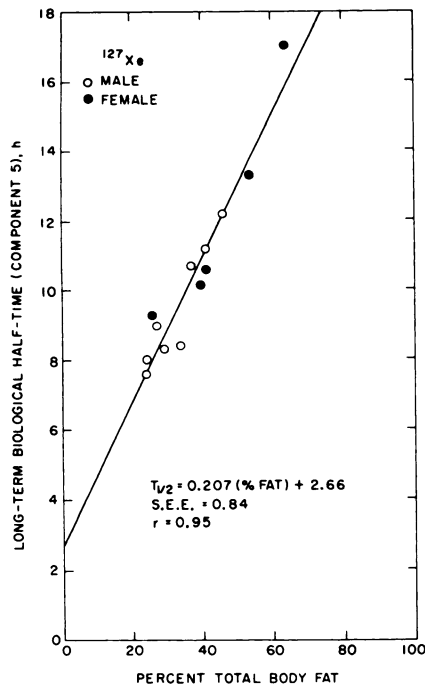


FIG. 6. Correlation of the long-term (component 5) biologic half-time with the percent total-body fat.

where

$Q_0$  = amount of gas in the tissue at start of gas washout,  $t = 0$ ;

$\lambda$  = rate constant,  $0.693/t_{1/2}$ ;

$t_{1/2}$  = time interval during which half the original gas in the tissue has cleared from the body;

$t$  = time.

Since the body is composed of tissues of varying

composition, with widely differing perfusion rates and partition coefficients, the TBR at time  $t$  becomes the sum of the retentions for the different tissue components

$$\text{TBR}(t) = \sum Q_i(t) = \sum Q_{0i}e^{-\lambda_i t},$$

where  $i$  is a particular tissue.

The results of this study, showing that the clearance of xenon can be described by a five-compartment model with half-times ranging from 22 sec to 17 hr (Table 2), are in general agreement with the work of Guillot and Giubileo (13) and Turkin and Moskalev (14). Guillot and Giubileo found five components of  $^{133}\text{Xe}$  clearance in nine subjects, following 1- to 3-min inhalations, with respective half-times of 36 sec, 2.5 min, 0.20 hr, 1.0 hr, and 5.33 hr. The last three values were obtained with a whole-body counter, consisting of a single 20-cm-diam  $\times$  10-cm-long NaI detector. They also measured the  $^{133}\text{Xe}$  activity in the inhaled and exhaled air. As might be expected from their measurements (with a single detector moved to different body locations) no spatial variation in the xenon distribution was found within the body following inhalation. On the other hand, Turkin and Moskalev fitted their clearance data with only four components, following  $^{133}\text{Xe}$  inhalation by four volunteers for periods of 0.5 to 66 hr in a 3.1 cu m exposure chamber. The average half-times assigned to the lungs, circulating blood, muscle, and fatty tissue, were respectively 30 sec, 30 sec,  $0.7 \pm 0.42$  hr, and  $6.2 \pm 1.8$  hr. In their subjects, a time of the order of 30 hr was required to reach saturation with xenon. They also

TABLE 3. DISTRIBUTION OF  $^{127}\text{Xe}$  IN THE BODY\*

Subject	TBR†, $\mu\text{Ci}$ at $t = 0$	Percent of total activity at $t = 0$ ‡			
		Component 2	Component 3	Component 4	Component 5
1	2.10		67.8	22.2	9.9
2	3.34		49.0	33.6	17.4
3(F)	3.84 (5.08)	24.2	42.6	30.0	3.2
4	3.95		—	71.7	28.3
5A	2.89		56.6	36.2	7.2
5B	11.17 (12.44)	10.3	48.7	28.3	12.6
6	42.34		—	63.9	36.1
7(F)	5.36		53.3	29.8	16.9
8(F)	3.24		45.8	39.5	14.8
9	4.30 (7.53)	43.6	11.1	30.9	14.4
10	3.37 (5.42)	37.9	33.9	16.4	11.8
11(F)	4.79 (6.07)	21.1	35.4	18.1	25.4
12(F)	3.16		—	56.7	43.3

\* Based on rebreathing a Xe-air mixture for 10 min.

† Total-body retention, based on components 3, 4, and 5 only; values in parentheses include component 2 as well.

‡ Start of xenon washout.

|| Values not computed for Subjects 4, 6, and 12 because of insufficient data in first 2 hr of washout.

observed that the  $^{133}\text{Xe}$  uptake was greater for a heavier, fatter subject than for a lighter, leaner one. Since they found no activity in blood samples taken 3 min after the end of exposure, they assumed that the xenon uptake and clearance in the blood proceeded at practically the same rate at which it exchanged in the lungs. Similar results with three or four compartments were obtained for krypton, which is less soluble in body tissues than xenon (14,20–22), and with five compartments for radon, which is more soluble than xenon (23). Krypton data from a related study in this laboratory also resulted in five compartments.

In the present study, too, the fastest component, No. 1 ( $t_{1/2} = 21.7 \pm 12.4$  sec), is believed to be due to gas clearance directly from the air spaces of the lungs immediately after the start of gas washout. This was in reasonable agreement with an average half-time of  $12.4 \pm 6.8$  sec calculated for the clearance of  $^{127}\text{Xe}$  from the lung air spaces of each subject. Since this calculation assumed the rapid dilution of lung air during each breath by the ratio of  $V_T/(FRC + \frac{1}{2}V_T)$ , the actual half-time would be expected to be somewhat greater than the calculated values because of mixing nonuniformities.

Clearance of xenon directly from recirculating blood, the most rapidly perfused tissue in the body, should result in two components: one representing the clearance of xenon dissolved in blood plasma, and the other the clearance of xenon attached to the hemoglobin molecules. The former component represents xenon that has transferred from venous blood to air at the rate of 90–95% per blood pass through the lungs (24). Its average half-time was calculated to be  $16.1 \pm 3.0$  sec, using predicted values of the cardiac output and blood volume for each subject. Since this value closely approximates that calculated above for xenon clearance directly from lung air, these two half-times were indistinguishable in this study and were therefore represented by a single component, No. 1—an observation also noted by Turkin and Moskalev (14).

Component 2, which appears to be diffusion-limited (25), is presumably associated with the removal of xenon attached to hemoglobin molecules in the circulating blood (6,26). Its average half-time of 3.05 min was similar to that determined by Schoenborn (personal communication) for the *in vitro* clearance of xenon from the hemoglobin molecule. Veall and Mallet (27) measured  $^{133}\text{Xe}$  clearance from the brain and also found two very similar components, with respective half-times of 24 sec and 5 min. They felt, however, that the faster one represented xenon clearance from the blood, while the slower one had no biologic significance. Component

3, with an average half-time of  $0.40 \pm 0.11$  hr, measured xenon clearance from resting muscle and lean body tissues, and compared very favorably with the value of  $0.27 \pm 0.12$  hr determined by Holzman, et al. (28) following intramuscular injection of  $^{133}\text{Xe}$  into the forearms of their subjects. Component 4, which is related to xenon solubility in fat (25), may indicate a substantial fat compartment not in adipose tissue, or a nonuniformity in the perfusion rates for adipose tissue.

The biologic half-time for the slowest component, No. 5, correlated significantly ( $r = 0.95$ ) with the percent total-body fat (Fig. 6). The relationship is

$$t_{1/2} = 0.207 (\% \text{ fat}) + 2.66,$$

when  $t_{1/2}$  is expressed in hours. The standard error of the estimate is 0.84.

The longer retention of xenon in adipose tissue, compared with other tissues, is directly related to its preferential solubility in fat. The tissue perfusion

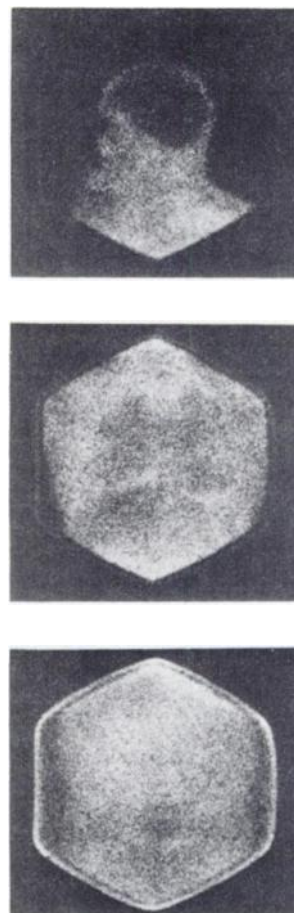


**FIG. 7.** Typical  $^{127}\text{Xe}$  distribution in the body ~30 min after rebreathing and washout of millicurie amounts in a ventilation study. Lateral head image shows xenon is located primarily in the circulating blood (top). In anterior chest (middle) and abdominal (bottom) images, xenon is located primarily in adipose tissue, as well as in the heart and other blood compartments. Note relatively dark lung fields in middle view.



rate is the rate-limiting step in the removal of xenon from this compartment, as well as from the fourth (25). Perfusion-limited gas clearance implies the assumption of a diffusion equilibrium between the tissues and the perfusing blood. This appears to be the case here, since the clearance rates, after 30 min of gas rebreathing, were essentially the same as those after 10 min (Table 5). Renkin (29) suggested that inert gases attain virtually complete equilibrium between tissues and blood during a single passage through the capillary bed. Adipose tissue appears to have a homogenous distribution of blood flow, as shown by the studies of Nielsen (30), who obtained good agreement between blood-flow rates measured directly in rabbits and those calculated from washout following the atraumatic injection of  $^{133}\text{Xe}$  into adipose tissue. On the other hand, blood flow per unit mass decreased significantly with the thickness of fatty tissue (31,32), so that the rate of gas transport would be expected to decrease with body-fat content. While intertissue diffusion also plays a significant role in gas exchange from adipose tissue, amounting to as much as 18% (33,34), the perfusion-controlled transport probably masked this effect here.

In a related study with  $^{79}\text{Kr}$ , typical profile distributions of the coincidence count were obtained on the whole-body counter. As the total-body activity

decreased between 1 hr and 24 hr, the relative distribution of krypton shifted from the chest region to the lower abdomen and thigh regions, areas of high fat content. This relative shift in the spatial distribution could not be measured with  $^{127}\text{Xe}$  because it is not a positron emitter, but similar results are probably implicit in the present study as well. The long-term retention of  $^{127}\text{Xe}$  in the body was observed with the scintillation camera following ventilation studies with millicurie amounts. Significant amounts of  $^{127}\text{Xe}$  were found in images of the head, chest region, and abdomen of patients ~30 min after completion of the studies (Fig. 7). In the head the xenon was located primarily in the circulating blood, whereas in the chest and abdomen the scintiscans showed xenon to be primarily in adipose tissue, as well as in the heart and other blood compartments. Significantly, the lungs were relatively devoid of radioactivity, while the surrounding areas contained measurable amounts of  $^{127}\text{Xe}$ .

The absolute amount of  $^{127}\text{Xe}$  retained in the body depends on such factors as: (A) its concentration in the air mixture; (B) duration of exposure to the xenon-air mixture; and (C) total-body fat. The first two factors were kept constant in this study. Enough  $^{127}\text{Xe}$  was introduced to the system so that approximately the same amount per liter was present in the lungs of all subjects, regardless of their

TABLE 4. DISTRIBUTION OF  $^{127}\text{Xe}$  IN THE LUNGS AND THE BODY\*

Subject	Average lung volume, liters	Total activity at $t = 0^\dagger$ , $\mu\text{Ci}$				
		Lungs	TBR $^\ddagger$	Component 5	$f   \times 10^{-3}$	$k   \times 10^{-3}$
1	3.2	13.47	2.10	0.208	1.34	3.46
2	2.9	—	3.34	0.582	—	—
3(F)	3.8	12.08	3.84	0.164	1.03	3.60
4	5.2	118.1§	3.95	1.12	0.92	2.36
5A	5.2	10.90	2.89	0.208	1.51	3.82
5B	5.1	18.57	11.17§	1.57	5.28	13.01§
6	5.1	872.1§	42.34§	15.3§	1.67	2.90
7(F)	3.5	21.68	5.36	0.905	3.35	6.35
8(F)	3.4	9.23	3.24	0.479	3.84	8.62
9	4.5	10.68	4.30	1.09	7.28	9.19
10	4.7	11.14	3.37	0.640	4.41	5.14
11(F)	1.9	13.73	4.79	1.54	8.32	4.41
12(F)	2.7	14.06	3.16	1.37	7.96	2.98
	Mean	13.55	3.66	0.822	3.91	4.80
	s.d.	3.85	0.91	0.516	2.77	2.31

\* Based on rebreathing a xenon-air mixture for 10 min.

$^\dagger$  Start of xenon washout.

$^\ddagger$  Total-body retention, based on components 3, 4, and 5 only.

$||$  Fraction of xenon in body at start of gas washout;  $f = \frac{\mu\text{Ci long-term TBR (comp. 5)}}{\mu\text{Ci total activity in lungs} + \text{TBR}}$ .

$||$  Ratio of the concentrations of xenon distributed between fatty tissues and air at start of xenon washout;

$$k = \frac{\mu\text{Ci long-term TBR (comp. 5)/kg BF}}{\mu\text{Ci lung activity/liter of lung volume}}$$

§ Values not included in calculating the means and standard deviations.

TABLE 5. EFFECT OF REBREATHING TIME

		Biologic half-time, $t_{1/2}$ , hr					
		Component 3		Component 4		Component 5	
Subject	Time, min	10	30	10	30	10	30
2		0.20	0.27	1.54	1.76	8.01	8.96
9		0.52	0.49	1.10	3.57	11.20	11.10
10		0.48	0.42	2.84	3.61	12.22	11.98
		Total activity at $t = 0$ , $\mu\text{Ci}$					
		Lungs		TBR*		Component 5	
Subject	Time, min	10	30	10	30	10	30
2		—	14.75	3.34	12.80	0.582	6.61
9		10.68	4.32	4.30	6.53	1.09	1.66
10†		11.14	0.27	3.37	2.30	0.640	0.39
		$f\ddagger \times 10^{-3}$		$k   \times 10^{-3}$			
Subject	Time, min	10	30	10	30		
2		—	24.0	—	72.4		
9		7.28	15.3	9.19	33.9		
10†		4.41	15.2	5.14	125.7		
	Mean	5.85	18.2	7.17	77.3		
	s.d.	2.03	5.1	2.86	46.1		

\* Total-body retention, based on Components 3, 4, and 5 only.

† Spirometer system leaked.

 $\ddagger$  Fraction of xenon in body at start of gas washout;  $f = \frac{\mu\text{Ci long-term TBR (comp. 5)}}{\mu\text{Ci total activity in lungs} + \text{TBR}}$ . $||$  Ratio of the concentrations of xenon distributed between fatty tissues and air at start of xenon washout; $k = \frac{\mu\text{Ci long-term TBR (comp. 5)/kg BF}}{\mu\text{Ci lung activity/liter of lung volume}}$ .

lung volumes. Consequently, except for Subjects 4 and 6, the total activity in the lungs varied only between 9.23 and 18.57  $\mu\text{Ci}$ , with an average value of  $13.55 \pm 3.85 \mu\text{Ci}$  (Table 4). When normalized for the subject's lung volume, the average concentration was  $3.95 \pm 1.80 \mu\text{Ci/liter}$ . Moreover, all subjects rebreathed the gas mixture for 10 min. The TBR values at the start of gas washout (the sum of the intercepts of components 3 to 5) were significantly less than the  $^{127}\text{Xe}$  activity in the lungs, which verifies the very rapid clearance from the lungs and circulating blood during the first 5 min measured with the scintillation camera.

Equilibrium was not attained during the short exposure times of this study. The rate of saturation of the body by  $^{127}\text{Xe}$  is a complex function of the tissue-to-blood partition coefficients and perfusion rates for the individual tissues. For short exposure times, an apparent equilibrium is reached for the blood and highly perfused lean tissues (14). However, true equilibration into the fat spaces, takes considerably longer, of the order of hours. The ratio  $k$  for the concentration of  $^{127}\text{Xe}$  distributed between fatty tis-

sues and air after rebreathing the xenon-air mixture for 10 min,\* was calculated in each case for component 5 in adipose tissue at the start of gas washout; it ranged from  $2.36 \times 10^{-3}$  to  $9.19 \times 10^{-3}$  (Table 4). As expected,  $k$  for Subjects 4 and 6, who rebreathed higher  $^{127}\text{Xe}$  concentrations than the rest, but for the same length of time, was similar to that of the others.

When the long-term TBR component (No. 5) is expressed as a fraction of the total  $^{127}\text{Xe}$  present in lungs and body at the start of gas washout after rebreathing the xenon-air mixture for 10 min, this fraction† varied from  $0.9 \times 10^{-2}$  to  $8.3 \times 10^{-2}$  and averaged  $4 \times 10^{-2}$  (Table 4). The concentration in adipose tissue would, of course, increase with exposure time until saturation is reached. Consequently, both the concentration ratios and xenon

$$* k = \frac{\text{Ci long-term TBR (component 5)/kg body fat}}{\mu\text{Ci lung activity/liter lung volume}}$$

$$\dagger f = \frac{\mu\text{Ci long-term TBR (component 5)}}{\mu\text{Ci total activity in lungs} + \text{TBR}}$$



fractions increased by factors of 11 and 3, respectively, as the rebreathing time was increased from 10 to 30 min (Table 5). The saturation/desaturation phases have been shown previously to be independent of the length of time of exposure, whereas the total amount of gas retained in the adipose tissue increased. This was also observed in our study (Table 5).

**Radiation dosimetry.** The radiation dose from a given administered activity of radioxenon will depend on (A) the relative volumes of the spirometry system and the average lung volume of the subject, (B) the length of time during which the subject rebreathes the xenon-air mixture prior to gas washout, and (C) the rate of gas washout from the lungs. In addition, as can be seen from this study, the percent total-body fat will be a factor bearing on the dose from the fraction of the total activity that leaves the body with a half-time greater than 2.7 hr (components 4 and 5). Calculations based on data from this study were performed using the "S" values of MIRD Pamphlet No. 11 (35). Values of S were chosen for the whole body as a source, and for the whole body, testes, ovaries, and bone marrow as target organs. A separate calculation for fat was made by dividing the whole-body dose by the fraction of whole-body fat and assuming a uniform body distribution of adipose tissue. Since this study has shown that the long-term distribution of radioxenon in the body is not uniform (Fig. 7), the MIRD approach should take this into account.

The estimated radiation dose, in mrad per mCi of  $^{127}\text{Xe}$  in the lungs at the start of gas washout, is shown as follows for a very lean subject (No. 1), an obese subject (No. 12), and an "average" subject:

	Very lean	Obese	Average
Total body	1.19	12.3	6.07
Testes	1.02	—	5.22
Ovaries	—	14.5	7.16
Bone marrow	1.59	16.5	8.13
Body fat	4.91	19.4	16.2

The dose from  $^{133}\text{Xe}$  would be ~19% greater for total body and body fat, ~85% greater for testes, 13% greater for ovaries, and ~49% greater for marrow.

#### SUMMARY

Five components for the clearance of  $^{127}\text{Xe}$  from the entire body were measured in vivo, with biologic half-times ranging from 22 sec to 17 hr (Table 6). The slowest component correlated highly with percent total-body fat, the half-time varying between 7.59 and 17.04 hr. After 10-min inhalations of a mix-

TABLE 6. SUMMARY OF  $^{127}\text{Xe}$  DISTRIBUTION PARAMETERS\*

Component	Biologic half-time, $t_{1/2}$	Distribution of activity at $t = 0^\dagger$		
		Body retention		Lungs + body %
		$\mu\text{Ci}$	%	
1	21.7 $\pm$ 12.4 sec	—	—	—
2	3.05 $\pm$ 1.72 min	1.82 $\pm$ 0.88	28.1	9.1
3	0.40 $\pm$ 0.11 hr	2.21 $\pm$ 1.46	34.1	11.0
4	2.71 $\pm$ 0.87 hr	1.63 $\pm$ 0.88	25.1	8.1
5	7.59 — 17.04 hr	0.82 $\pm$ 0.52	12.7	4.1
Total retention in body		6.48	100.0	32.3
Total distributed in lungs		13.55		67.6
Total in body + lungs		20.03		100

\* Based on rebreathing a xenon-air mixture for 10 min.

† Start of xenon washout.

ture of  $^{127}\text{Xe}$  and air, approximately one-third of the total  $^{127}\text{Xe}$  was transferred to the body tissues, extrapolated back to the start of gas washout. Of this amount, ~13% was associated with the slowest component.

#### ACKNOWLEDGMENT

This work was carried under contract E(30-1)-16 with the U.S. Energy Research and Development Administration.

We thank W. H. Harold and W. P. Lehman for their help in conducting the experiments, A. Ansari for obtaining part of the scintillation-camera data, T. F. Prach for preparing and counting the sampling bulbs, M. J. Stravino and A. F. LoMonte for the whole-body counter measurements, and H. R. Pate for the computer computations.

#### FOOTNOTES

\* Brookhaven Linac Isotope Producer (BLIP), Brookhaven National Lab., Upton, N.Y.

† Ventil-Con, RADX Corp., Houston, Texas.

‡ Series 110, Ohio-Nuclear Inc., Solon, Ohio.

#### REFERENCES

1. WAGNER HN JR: The use of radioisotope techniques for the evaluation of patients with pulmonary disease. *Am Rev Respir Dis* 113: 203-218, 1976
2. ARNOT RN, CLARK JC, GLASS HI: Investigation of  $^{127}\text{Xe}$  as a tracer for the measurement of regional cerebral blood flow. In Russell RWR, ed, *Proc 4th Intern Symp on the Regulation of Cerebral Blood Flow*, London, Pitman, 1971, pp 16-21
3. HOFFER PB, HARPER PV, BECK RN, et al.: Improved xenon images with  $^{127}\text{Xe}$ . *J Nucl Med* 14: 172-174, 1973
4. GODDARD BA, ACKERY DM: Xenon-133,  $^{127}\text{Xe}$ , and  $^{135}\text{Xe}$  for lung function investigations: A dosimetric comparison. *J Nucl Med* 16: 780-786, 1975
5. LAWRENCE JH, LOOMIS WF, TOBIAS CA, et al.: Preliminary observation on the narcotic effect of xenon, with a review of values for solubilities of gases in water and in oils. *J Physiol* 105: 197-204, 1946

6. CONN HL JR: Equilibrium distribution of radioxenon in tissue: xenon-hemoglobin association curve. *J Appl Physiol* 16: 1065-1070, 1961
7. ANDERSEN AM, LADEFOGED J: Relationship between hematocrit and solubility of  $^{135}\text{Xe}$  in blood. *J Pharm Sci* 54: 1684-1685, 1965
8. YEH S-Y, PETERSON RE: Solubility of krypton and xenon in blood, protein solutions, and tissue homogenates. *J Appl Physiol* 20: 1041-1047, 1965
9. ISBISTER WH, SCHOFIELD PF, TORRANCE HB: Measurement of the solubility of xenon-133 in blood and human brain. *Phys Med Biol* 10: 243-250, 1965
10. MUEHLBAECHER CA, DEBON FL, FEATHERSTONE RM: Further studies on the solubilities of xenon and cyclopropane in blood and protein solutions. *Mol Pharmacol* 2: 86-89, 1966
11. ANDERSEN AM, LADEFOGED J: Partition coefficient of  $^{135}\text{Xe}$  between various tissues and blood in vivo. *Scand J Clin Lab Invest* 19: 72-78, 1967
12. KITANI K: Solubility coefficients of  $^{86}\text{Krypton}$  and  $^{135}\text{Xenon}$  in water, saline, lipids, and blood. *Scand J Clin Lab Invest* 29: 167-172, 1972
13. GUILLOT P, GIUBILEO M: Mésures pour l'évaluation des doses en cas d'inhalation de  $^{135}\text{Xe}$ . Paper presented at First European Congress on Radioprotection, Menton, Oct 9-11, 1968. (Rapport No. 29-IP/0140/N-Comptes Rendus, p 289)
14. TURKIN AD, MOSKALEV YI: Kinetics and distribution of xenon-133 and krypton-85 in the human body. In Stanley RE, Moghissi AA, eds, *Noble Gases*, U.S. Energy Research and Development Administration report, CONF. 730 915, 1973, pp 472-483
15. COHN SH, DOMBROWSKI CS, PATE HR, et al.: A whole-body counter with an invariant response to radionuclide distribution and body size. *Phys Med Biol* 14: 645-658, 1969
16. COHN SH, DOMBROWSKI CS: Absolute measurement of whole body potassium by gamma-ray spectrometry. *J Nucl Med* 11: 239-246, 1970
17. SHUKLA KK, ELLIS KJ, DOMBROWSKI CS, et al.: Physiological variation of total-body potassium in man. *Am J Physiol* 224: 271-274, 1973
18. BERMAN M, SHAHN E, WEISS MF: The routine fitting of kinetic data to models: A mathematical formalism for digital computers. *Biophys J* 2: 275-287, 1962 (SAAM-25 is the 1974 version of the code)
19. KETY SS: The theory and applications of the exchange of inert gas at the lungs and tissues. *Pharmacol Rev* 3: 1-41, 1951
20. TOBIAS CA, JONES HB, LAWRENCE JH, et al.: The uptake and elimination of krypton and other inert gases by the human body. *J Clin Invest* 28: 1375-1385, 1949
21. LESSER GT, ZAK G: Measurement of total body fat in man by the simultaneous absorption of the two inert gases. *Ann NY Acad Sci* 110: 40-54, 1963
22. HYTTEN FE, TAYLOR K, TAGGART N: Measurement of total body fat in man by absorption of  $^{86}\text{Kr}$ . *Clin Sci* 31: 111-119, 1966
23. HARLEY JH, JETTER E, NELSON N: Elimination of radon from the body. U.S. Atomic Energy Commission report HASL-32, Mar 20, 1958
24. BASS H: Assessment of regional pulmonary function with radioactive gases. In Holman BL, Lindeman JF, eds, *Progress in Nuclear Medicine*, vol 3. Baltimore, University Park Press, 1973, pp 67-84
25. SUSSKIND H, ATKINS HL, COHN SH, et al.: The kinetics of total body retention and clearance of xenon and krypton after inhalation. *Proc 29th Ann Conf Eng Med Biol* 18: 225, 1976
26. SCHOENBORN BP: Binding of xenon to horse haemoglobin. *Nature* 208: 760-762, 1965
27. VEALL N, MALLET BL: Regional cerebral blood flow determination by  $^{135}\text{Xe}$  inhalation and external recording: The effect of arterial recirculation. *Clin Sci* 30: 353-369, 1966
28. HOLZMAN GB, WAGNER HN JR, IIO M, et al.: Measurement of muscle blood flow in the human forearm with radioactive krypton and xenon. *Circulation* 30: 27-34, 1964
29. RENKIN EM: Capillary permeability to lipid-soluble molecules. *Am J Physiol* 168: 538-545, 1952
30. NIELSEN SL: Measurement of blood flow in adipose tissue from the washout of xenon-133 after atraumatic labelling. *Acta Physiol Scand* 84: 187-196, 1972
31. LARSEN OA, LASSEN N-A, QUADE F: Blood flow through human adipose tissue determined with radioactive xenon. *Acta Physiol Scand* 66: 337-345, 1966
32. LESSER GT, DEUTSCH S: Measurement of adipose tissue blood flow and perfusion in man by uptake of  $^{86}\text{Kr}$ . *J Appl Physiol* 23: 621-630, 1967
33. PERL W, RACKOW H, SALANITRE E, et al.: Intertissue diffusion effect for inert fat-soluble gases. *J Appl Physiol* 20: 621-627, 1964
34. MADSEN J, MALCHOW-MØLLER A, WALDORFF S: Continuous estimation of adipose tissue blood flow in rats by  $^{135}\text{Xe}$  elimination. *J Appl Physiol* 39: 851-856, 1975
35. SNYDER WS, FORD MR, WARNER GG, et al.: "S" absorbed dose per unit cumulated activity for selected radionuclides and organs. MIRD Pamphlet No. 11, Society of Nuclear Medicine, New York, 1975